Boletim da Sociedade Astronômica Brasileira, **35**, no. 1, 313-316

Photometric characterization of SPARC4

W. Schlindwein[1], J. C. N. Campagnolo[2], E. Martioli[3], L. Almeida[3], L. Andrade[3], D. Bernardes[1], F. Falkenberg[1], L. Fraga[3], F. J. Jablonski[1], A. C. Mattiuci[1], & C. V. Rodrigues[1]

[1] Instituto Nacional de Pesquisas Espaciais (INPE)
[2] Centro Federal de Educação Tecnológica Celso Suckow da Fonseca (CEFET/RJ)
[3] Laboratório Nacional de Astrofísica (LNA)
e-mail: wagner.schlindwein@inpe.br

Abstract. The instrument Simultaneous Polarimeter and Rapid Camera in Four Bands (SPARC4) is being commissioned in the 1.6 m telescope of the Pico dos Dias Observatory (OPD). It is the result of a partnership between *Instituto Nacional de Pesquisas Espaciais* (INPE) and *Laboratório Nacional de Astrofísica* (LNA). In this work, we present the photometric characterization of SPARC4, such as its field distortions and signal-to-noise ratio. We will also discuss the photometric calibration procedure done through astronomical catalogs (e.g. Gaia DR3). Finally, we discuss the quality and consistency of the transformations of the natural system to the Sloan Sky Digital Survey (SDSS) griz standard system, given that the SPARC4 bands were designed to be similar to those of SDSS.

Resumo. O instrumento *Simultaneous Polarimeter and Rapid Camera in Four Bands* (SPARC4) está a ser comissionado no telescópio de 1.6 m do Observatório do Pico dos Dias (OPD). Ele é o resultado de uma parceria entre o Instituto Nacional de Pesquisas Espaciais (INPE) e o Laboratório Nacional de Astrofísica (LNA). Nesse trabalho apresentamos a caracterização fotométrica da SPARC4, como suas distorções de campo e relação sinal-ruído. Também discutiremos o procedimento de calibração fotométrica feito através de catálogos astronômicos (por exemplo, Gaia DR3). Por fim, discutimos a qualidade e consistência das transformações do sistema natural para o sistema padrão griz do *Sloan Sky Digital Survey* (SDSS), visto que as bandas da SPARC4 foram projetadas para serem semelhantes às do SDSS.

Keywords. Instrumentation: photometers – Techniques: photometric – Methods: observational

1. Introduction

The *Instituto Nacional de Pesquisas Espaciais* (INPE), in partnership with the *Laboratório Nacional de Astrofísica* (LNA), is developing a new astronomical instrument called the Simultaneous Polarimeter and Rapid Camera in Four Bands (SPARC4, Rodrigues et al. 2012, 2024), which will be installed on the 1.6 m telescope at the Pico dos Dias Observatory (OPD).

The SPARC4 instrument is characterized by the simultaneous acquisition of images in four broad bands in the optical region of the electromagnetic spectrum (similar to the g, r, i and z bands of the Sloan Sky Digital Survey - SDSS, Gunn et al. 1998), for a temporal resolution of up to tenths of a second and for two modes of operation: photometry (this work) and polarimetry (Mattiuci et al. 2024). This combination makes SPARC4 a very versatile instrument, with a wide range of scientific applications, so the expectation is that there will be great demand for observations with this instrument. SPARC4 represents a significant improvement in the instrumentation made available to OPD users and an increase in the productivity of this observatory is expected.

The machining of the instrument was completed in 2020. Some tests were carried out in 2021 and 2022, but the integration of the instrument was only completed in the second half of 2022 so that the instrument's first light occurred in November 2022. In 2023, the instrument entered the final commissioning phase, and between June and July, the Brazilian astronomical community carried out scientific verification of SPARC4.

2. Observations and data reduction

In November 2022, the first light occurred with the integrated instrument, where SPARC4 was installed on the 1.6 m telescope at the OPD. Already in the first light, SPARC4 obtained high-quality data. During 2023, several observational missions were carried out where the instrument was commissioned. In this work, we will show the analysis of a set of data obtained on May 3, 2023 in photometric mode.

The SPARC4 project is also developing a reduction software based on the ASTROPOP package (Campagnolo 2019; Campagnolo et al. 2024), which uses the Python programming language and provides routines for the complete reduction of photometric or polarimetric data. The commissioning data of SPARC4 cameras has been reduced using ASTROPOP. This reduction was validated through comparison with IRAF (Image Reduction and Analysis Facility).

3. Characterization

3.1. Field distortions

All optical systems suffer from aberrations and field distortions of some kind. The mapping of these distortions and subsequent correction is essential for high-precision photometry and astrometry. We have performed distortion mapping of all channels.

Images of a rich field with coordinates RA=18:40:50 and DEC=−06:47:00 were obtained with SPARC4 and used to determine the field distortions of the channels. 100 images were collected with an exposure time of 2 s with a read-out rate of 1 MHz and a pre-amplifier gain of 2. All data were bias subtraction and flat-field corrected prior to distortion correction and stacked into a single image for each channel; the astrometry routine from the ASTROPOP package was used, it uses Astrometry.net[1] (Lang et al. 2010) to calculate the astrometric solution. A third-order

[1] https://nova.astrometry.net/

polynomial was performed on these data to determine the field distortion by fitting the residuals from the plate solution. A total of 27, 42, 27 and 24 stars were used to fit this polynomial, respectively, for channels 1 (g), 2 (r), 3 (i) and 4 (z), with the rms of the residuals being 80, 31, 34 and 32 mas. The results are shown in Fig. 1. The distortions increase towards the edges of the field with a maximum value at the edges of ~ 5 arcsec in all channels.

3.2. Noise characterization

We used the same dataset from Section 3.1 to characterize the SPARC4 photometry noise. ASTROPOP was used to calculate the aperture photometry of the stars detected at 100σ above the background in each channel. ASTROPOP uses SEP (Barbary 2016) for aperture photometry. The ASTROPOP error (aperture photometry error from SEP) is:

$$\mathrm{FLUXERR} = \sqrt{\sum_{i\in\mathcal{A}}\left(\sigma_i^2 + \frac{p_i}{g_i}\right)} \quad (1)$$

where $\mathcal{A}$ is the set of pixels defining the photometric aperture, σ_i is the standard deviation of noise (in ADU) estimated from the local background, p_i is the measurement image pixel value subtracted from the background, and g_i is the effective detector gain in e^-/ADU at pixel i.

The data points in Fig. 2 show 173, 556, 559 and 472 stars that were detected for channels 1 (g), 2 (r), 3 (i) and 4 (z), respectively. A circular aperture with a radius of 6 pixels was used. SPARC4 has good signal-to-noise ratio. The magnitude calibration procedure will be described in Section 3.3. With the noise characterization, we created a preliminary version of an Exposure Time Calculator (ETC) that is published on the LNA website [2]. A full version will be available in the future.

3.3. Photometric calibration

It is important to calibrate the SPARC4 photometric system to allow comparison with results obtained from other observatories and instruments. To do this, we will use the images themselves for calibration, eliminating the effects of sky variations.

In our procedure, we first perform a match between the objects in our images and the GaiaDR3 catalog (Gaia Collaboration et al. 2016, 2023). Subsequently, transformations of the G, G_{BP} and G_{RP} magnitudes from GaiaDR3 to the $griz$ magnitudes of SDSS12 (Alam et al. 2015) through the photometric relationships described by Riello et al. (2021). We apply sigmaclip filtering to eliminate outlines. Finally, we calculate the offset factor by calculating the median deviation between the instrumental and GaiaDR3 magnitudes. This simple offset gives a good photometric calibration for the fields, yielding an uncertainty in magnitude better than 0.1 mag in the worst case.

Using the photometry of the objects obtained in Section 3.2 and applying the procedure described previously, we obtain Fig. 3. The offset values obtained are 24.323 ± 0.003 mag, 25.029 ± 0.003 mag, 24.137 ± 0.002 mag and 23.567 ± 0.005 mag for channels 1 (g), 2 (r), 3 (i) and 4 (z), respectively. These values were added to the instrumental magnitudes to obtain the calibrated magnitudes in Fig. 2. As we can see in Fig. 3, the correlation between instrumental and GaiaDR3 magnitudes is very good and produces an adequate calibration of our data.

[2] https://www.gov.br/lna/pt-br/composicao-1/coast/obs/opd/instrumentacao/instrumentos-e-detectores

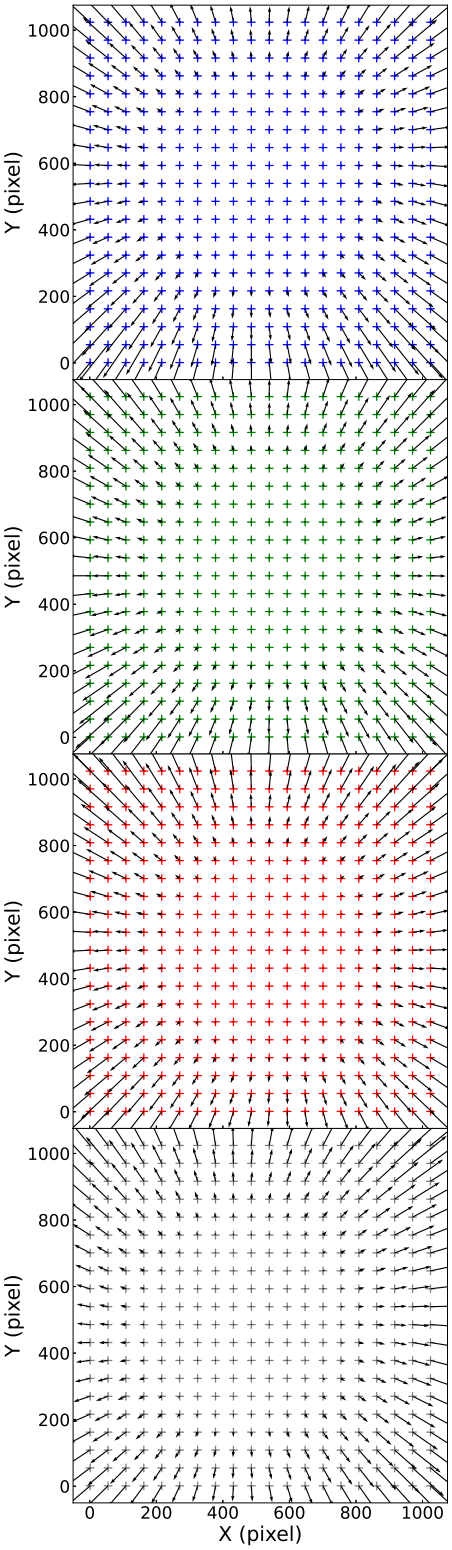

Figure 1. Third-order polynomial solution of the SPARC4 field distortion. The residuals of the fit are plotted as vectors for a 20×20 grid of points for all channels. The panels with blue, green, red and gray crosses represent channels 1 (g), 2 (r), 3 (i) and 4 (z), respectively. The crosses signify actual grid position, and vector magnitude and direction show distortion at that point. The coordinate system origin is at the center of the chip (512, 512). The pixel scale ~ 0.34 arcsec pixel^{-1} for all channels. We note that the scaling has been modified showing a residual vector zoom of 10× to give the reader a clearer understanding of distortion in the center.

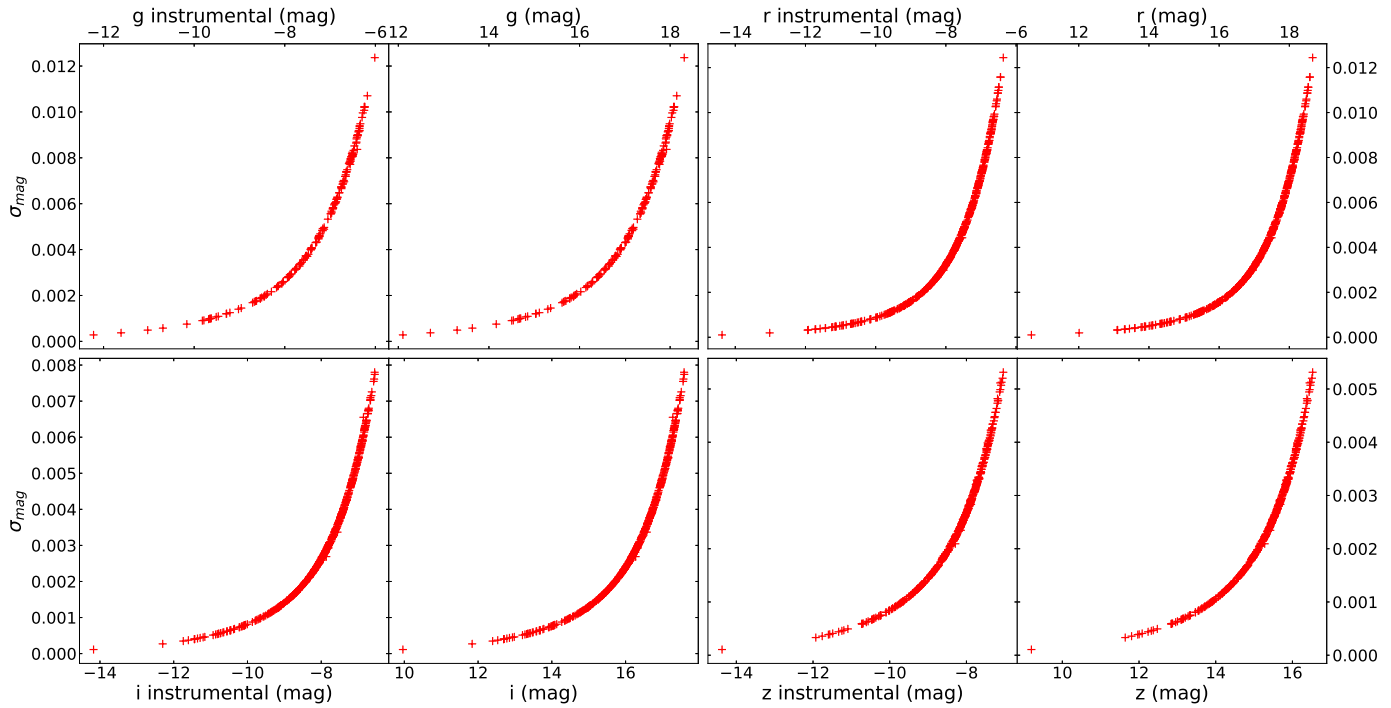

Figure 2. σ_{mag} versus magnitude plot of the measured noise performance of the SPARC4 instrument for all channels. The instrumental magnitude of each star in the plot is $-2.5\log(\text{flux})$. The procedure described in Section 3.3 was used to calibrate the magnitudes. We used a rich field (RA=18:40:50 and DEC=−06:47:00) in this analysis.

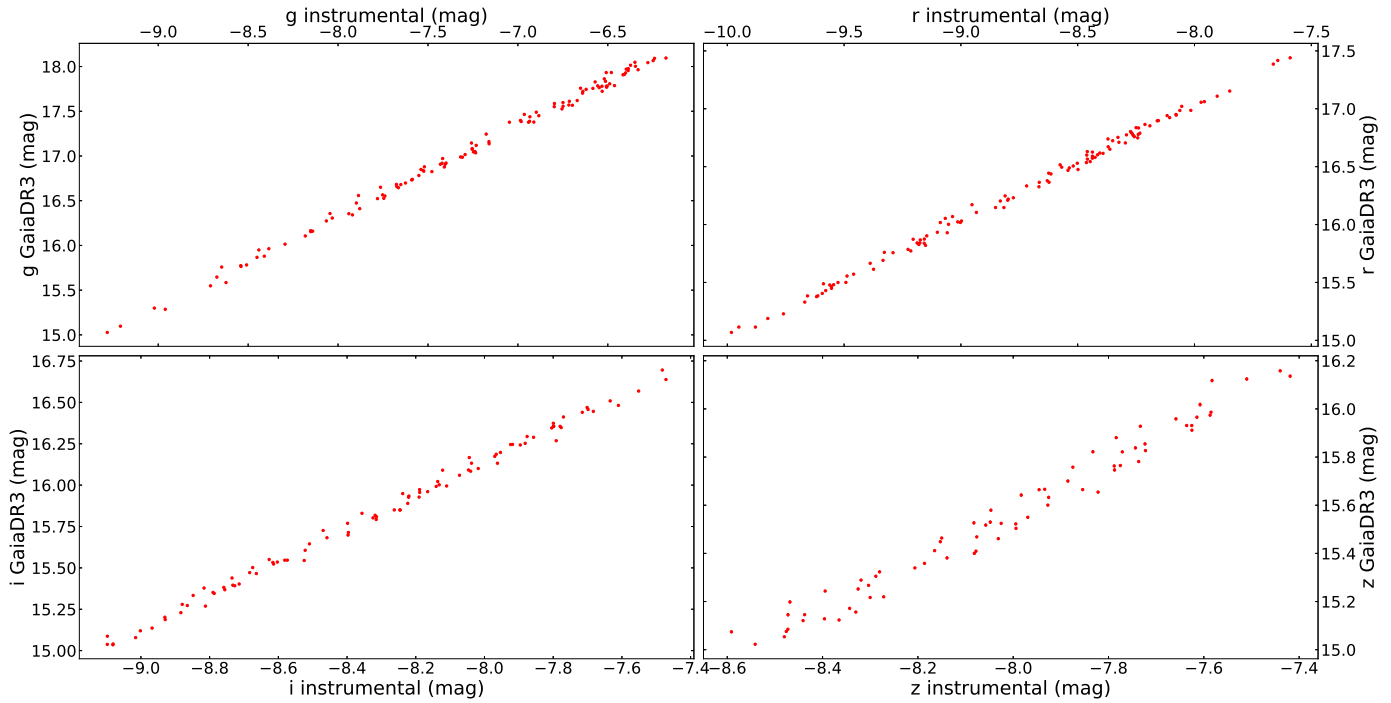

Figure 3. GaiaDR3 magnitudes versus instrumental magnitudes for all channels of SPARC4. We used a rich field (RA=18:40:50 and DEC=−06:47:00) in this analysis.

3.4. SPARC4 griz X SDSS griz

An interesting question to ask is whether the SPARC4 *griz* magnitudes are similar to the SDSS *griz* magnitudes. If so, the procedure described in Section 3.3 is valid; otherwise, it is necessary to estimate the photometric relationships between these two systems.

For these tests, we use the standard stars in the *ugriz* system that can be observed from the southern hemisphere (Smith et al. 2005). The observed field has coordinates of RA=11:59:56 and DEC=−59:55:52. Hundreds of images were collected and combined to produce a stacked image with an exposure time of 600 s. All data were bias subtraction and flat-field corrected. ASTROPOP was used to calculate the aperture photometry of

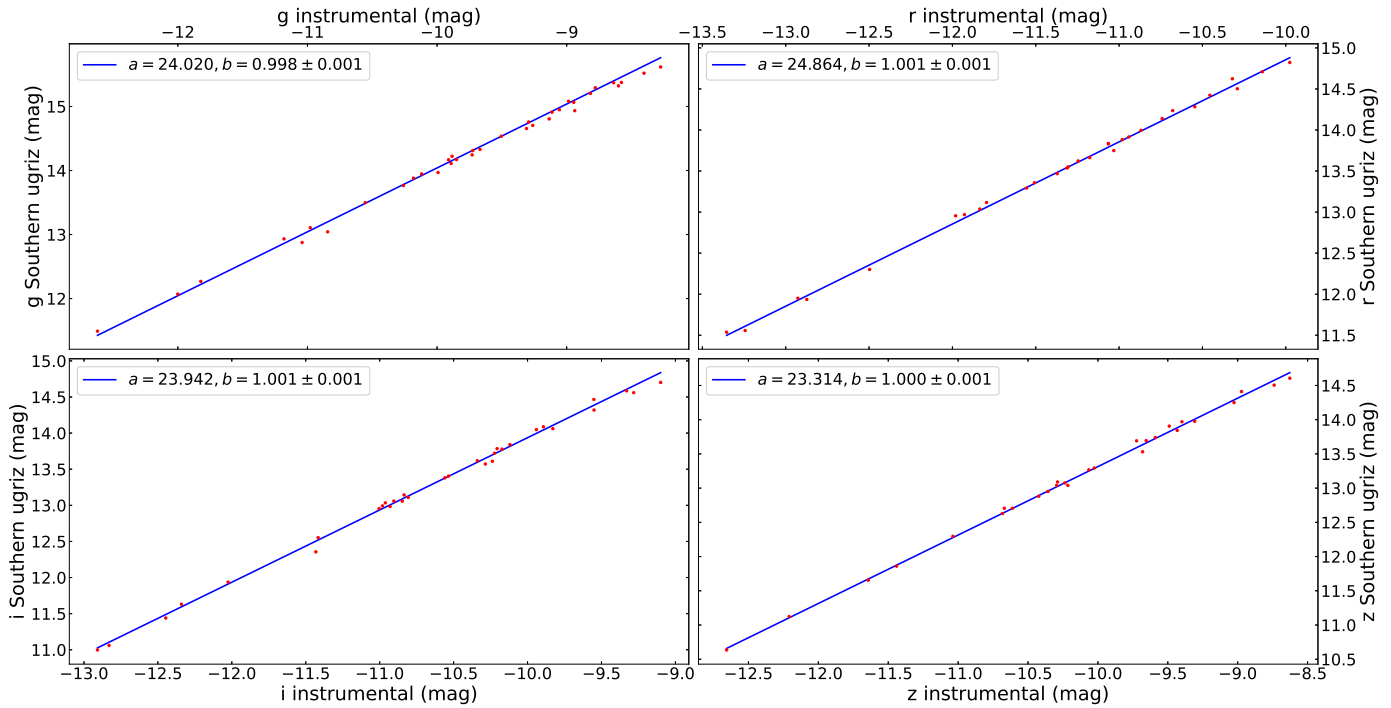

Figure 4. Southern standard magnitudes versus instrumental magnitudes for all channels of SPARC4. Blue lines are the best fit. The best-fit coefficient values are shown in the body of the image. We used a field with SDSS standard stars (RA=11:59:56 and DEC=−59:55:52) in this analysis.

the stars. A circular aperture with a radius of 6 pixels was used. A procedure analogous to that described in Section 3.3 was performed, but using the SDSS Southern standard instead of GaiaDR3. A total of 45, 44, 44 and 45 standard stars was identified in the field for channels 1 (g), 2 (r), 3 (i) and 4 (z), respectively, but 36, 30, 32 and 28 stars remained after sigmaclip filtering. The offset values obtained are 24.020 ± 0.064 mag, 24.864 ± 0.034 mag, 23.942 ± 0.045 mag and 23.314 ± 0.032 mag for channels 1 (g), 2 (r), 3 (i) and 4 (z), respectively. The results are shown in Fig. 4 as red dots. The blue line represents the fit of the best line by fixing the linear coefficient (a) as the offset value and the fit of the angular coefficient (b) taking into account the uncertainties in the measurements. The angular coefficients of the best fit are shown in the body of Fig. 4, and are unity within the uncertainties. This indicates that the SPARC4 *griz* magnitudes are very similar to the SDSS *griz* magnitudes.

A complete analysis will be performed taking into account the color indices, where we will follow the method described by Jablonski et al. (1994).

4. Conclusions and perspectives

We photometrically characterize the SPARC4 instrument, presenting in this work (i) the field distortions, which increase toward the edge of the field and have a maximum value of ∼ 5 arcsec in all channels; (ii) the signal-to-noise ratio obtained with SPARC4 is within the expected range, demonstrating that the instrument does not have any issues regarding throughput in all channels; (iii) a procedure for photometric calibration with uncertainties in magnitudes better than 0.1 mag in the worst case, which uses the images themselves to perform the calibrations through the GaiaDR3 catalog; and (iv) that the SPARC4 *griz* magnitudes are very similar to the SDSS *griz* magnitudes. To complete this work, there are more datasets obtained during the commissioning of the instrument that need to be analyzed and therefore produce a more robust characterization of SPARC4. An article that will describe the methods and results is being prepared to be published in 2024.

Acknowledgements. The SPARC4 project is funded by Finep (Proc. 0/1/16/0076/00), Agência Espacial Brasileira (AEB), Fapesp (Proc. 2010/01584-8), Fapemig, CNPq, and INCT-A. WS thanks CNPq (Proc. 300343/2022-1). EM acknowledges funding from FAPEMIG (APQ-02493-22) and CNPq for a research productivity grant number 309829/2022-4. ACM thanks FINEP (0/1016/0076/00). CVR thanks CNPq (Proc. 310930/2021-9). Based on observations made at the Observatório do Pico dos Dias/LNA (Brazil). We thank to the OPD staff for the technical support during the commissioning runs.

References

Alam S., Albareti F. D., Allende Prieto C., Anders F., Anderson S. F., Anderton T., Andrews B. H., et al., 2015, ApJS, 219, 12
Barbary K., 2016, JOSS, 1, 58.
Campagnolo J. C. N., 2019, PASP, 131, 024501
Campagnolo J. C. N., et al., 2024, BoSAB, this volume
Gaia Collaboration, Prusti T., de Bruijne J. H. J., Brown A. G. A., Vallenari A., Babusiaux C., Bailer-Jones C. A. L., et al., 2016, A&A, 595, A1
Gaia Collaboration, Vallenari A., Brown A. G. A., Prusti T., de Bruijne J. H. J., Arenou F., Babusiaux C., et al., 2023, A&A, 674, A1
Gunn J. E., Carr M., Rockosi C., Sekiguchi M., Berry K., Elms B., de Haas E., et al., 1998, AJ, 116, 3040
Jablonski F., Baptista R., Barroso J., Gneiding C. D., Rodrigues F., Campos R. P., 1994, PASP, 106, 1172
Lang D., Hogg D. W., Mierle K., Blanton M., Roweis S., 2010, AJ, 139, 1782
Mattiuci A. C., et al., 2024, BoSAB, this volume
Riello M., De Angeli F., Evans D. W., Montegriffo P., Carrasco J. M., Busso G., Palaversa L., et al., 2021, A&A, 649, A3. https://gea.esac.esa.int/archive/documentation/GDR3/Data_processing/chap_cu5pho/cu5pho_sec_photSystem/cu5pho_ssec_photRelations.html
Rodrigues C. V., Taylor K., Jablonski F. J., Assafin M., Carciofi A., Cieslinski D., Costa J. E. R., et al., 2012, SPIE, 8446, 844626
Rodrigues C. V., et al., 2024, BoSAB, this volume
Smith J. A., Allam S. S., Tucker D. L., Stute J. L., Rodgers C. T., Stoughton C., Beers T. C., et al., 2005, AAS. https://www-star.fnal.gov/Southern_ugriz/New/index.html